

## Design of Dry Friction Damper to Reduce Vibration Impacts to Circuit Cards at Critical Frequencies

Igor Kovtun<sup>1\*</sup>, Andrii Goroshko<sup>2</sup>, Svitlana Petrashchuk<sup>1</sup>

<sup>1</sup> Department of Art and Project Graphics, Khmelnytsky National University, 11 Institutaska Str., 29016 Khmelnytsky, Ukraine

<sup>2</sup> Department of Physics and Electrical Engineering, Khmelnytsky National University, 11 Institutaska Str., 29016 Khmelnytsky, Ukraine

\* Corresponding author's e-mail: kovtunih@khnmu.edu.ua

### ABSTRACT

The paper is focused on providing strength and stiffness for circuit cards exposed to vibration at critical frequencies. Since the dry friction damping is more effective than viscous damping and in case when application of viscous dampers is restricted by electronic package design the dry friction damper is proposed to be embedded to design of enclosure case in order to reduce oscillation amplitudes of circuit cards at critical frequencies. Dry friction damper produces dissipative forces – non-elastic resistance forces due to friction in kinematic pairs undergoing oscillations. The mathematical model has been developed for estimation of maximal dynamic stress and deflection in critical cross-section of circuit card with embedded dry friction damper at critical frequencies. Developed mathematical model specifies minimal limit value for stiffness of dry friction damper, which is used in engineering calculations to determine its geometric parameters. Design of dry friction damper is introduced by semi-elliptical beam with rectangular profile. The effectiveness of dry friction damper to reduce dynamic stress and deflection in circuit cards has been analytically proved and experimentally testified.

**Keywords:** dry friction damper, circuit card, oscillatory system, vibration, critical frequency, resonance, dynamic force, stress, deflection.

### INTRODUCTION

Circuit cards (CC) being the most critical units in any electronic package appear to be highly vulnerable to external mechanical impacts due to their relatively low strength parameters. The highest risk is represented by dynamic impacts such as shocks and vibration, which unlike static or even cyclic mechanical impacts produce considerably higher stress in the body of CC.

The most attention in publications discussing strength problems in electronic engineering is driven to the circuit cards. One of the most popular ways to analyze stress in circuit cards has been demonstrated in many publications by using the numerical analysis based on finite element method. In particular: in paper [1] it is used

in micromechanical model to describe elastic behavior of CC and predict its elastic bending and shear responses under static load though; in [2] – for dynamic analysis of multi-layered circuit card; in [3] – for stress analysis in microelectronic circuits subjected to static load; in [4] – for analysis of the dynamic response of circuit card assembly due to a board-level drop-shock, with the ultimate intention of establishing the maximum magnitude of stress, where circuit card was modeled as a spring-mass system and then as a beam supported at its two ends and subjected to a half-sine shock; in [5] – to analyze the CC vibration behaviors and stress development mechanisms in large size plastic ball grid array chip packaging, which was tested and analyzed under random vibration to access its application feasibility on satellite

electronics. Other publications are focused on ways for vibration reduction and suppression. In [6] a viscous damper with controller force to decrease the average of maximum displacement is represented as single and multiple mass dampers. In [7] particle damping is represented as an effective method of passive vibration control, the prediction of particle damping performed by using neural network is here studied. All these and many other methods and results, obtained when analyzing stress and strain conditions in circuit cards, gain certain effect and application, nevertheless the approach represented in this paper differs in its performance.

Results of the previous research published in [8, 9], confirming results represented in publications mentioned above, emphasized that dynamic forces are very likely to transmit through the enclosure case to circuit cards installed inside. These forces increase manifold and reach ultimate strength of circuit cards as they are passing resonant oscillation. Previous vibration tests on bearing enclosure cases conducted in [8] indicated increasing strain transmission to circuit cards inside the carcasses with decreasing stiffness of their side walls. Such effect can be explained by reducing dry friction damping produced by mutual displacement of contacting parts, which exceeds viscous damping in materials of these parts. Increasing vibration transmission is also observed when carcass is set on the shaker through elastic (soft) spacer. Another experimental research testified that embedding elastic and dissipative joint in the fixtures of circuit cards was ineffective to decrease vibration transmission since having insufficient effect on critical section of circuit cards, which, as previous research [10] had demonstrated, is the central section of circuit card that exhibit maximal stress and deflection for the main mode of oscillation at the first critical frequency. Vibration examination of electronic packages revealed that the highest vibration transmission especially in resonant conditions is observed for the circuit cards [9] inside the enclosure case unlike its other parts, such as case walls, which oscillations are not critical for their strength.

Represented research develops the general idea of stress and strain reduction in bearing structures of electronic packages on various levels of structural complexity through creation and modification of elastic and dissipative joints between parts of these structures, which appear to be the cause and the links for destructive

strain transmission as inside so outside of these structures subjected to static, cyclic and dynamic forces. The paper is focused on providing strength for circuit cards exposed to vibration at critical frequencies what is achieved by reducing dynamic stress and deflection in critical section of circuit cards by embedding elastic and dissipative joint introduced by dry friction damper between circuit card and enclosure case. Application of such proposal, which effectiveness is explained by mathematical modeling, simulation and experimental verification, represents the novelty of represented research.

### OSCILLATORY MODEL OF CIRCUIT CARD WITH DRY FRICTION DAMPER AT CRITICAL FREQUENCIES

Since the dry friction damping is more effective than viscous damping in materials and in case when application of viscous dampers is restricted by electronic package design the dry friction damper (DFD) is proposed to be embedded to design of enclosure case (Fig. 1a) in order to reduce oscillation amplitudes transmitted to circuit cards. DFD produces dissipative forces – non-elastic resistance forces due to friction in kinematic pairs undergoing oscillations [11]. DFD design is introduced by semi-elliptical beam with rectangular profile. The oscillatory model of circuit card with DFD is shown in Fig. 1b.

Circuit card is represented by two-supported weightless prismatic beam with single concentrated mass. The beam is supported by the pinned support O' providing one degree of freedom and roller support O'' providing two degrees of freedom. These supports transmit dynamic force to CC. Such model is justified in [9, 10] as such that reproduces highest level of maximal dynamic stress and deflection in CC. DFD as semi-elliptical beam has rigid joint with center of CC and movable joints with enclosure case by two clutches, which make the kinematic friction pairs for both ends of DFD.

In inertial frame of reference marked as 0 (Fig. 1) oscillation of the mass  $m$  progresses with acceleration  $z_1''$ , produced by kinematic excitation from ends of the circuit card, to which dynamic force is applied and which undergo vertical motion with given acceleration  $z_0''$ . Here  $z_0$  or  $z_0(t) = Z_0 \sin(\omega t + \varphi)$  stands for function of harmonic oscillation generated by a shaker along  $Z$  axis,

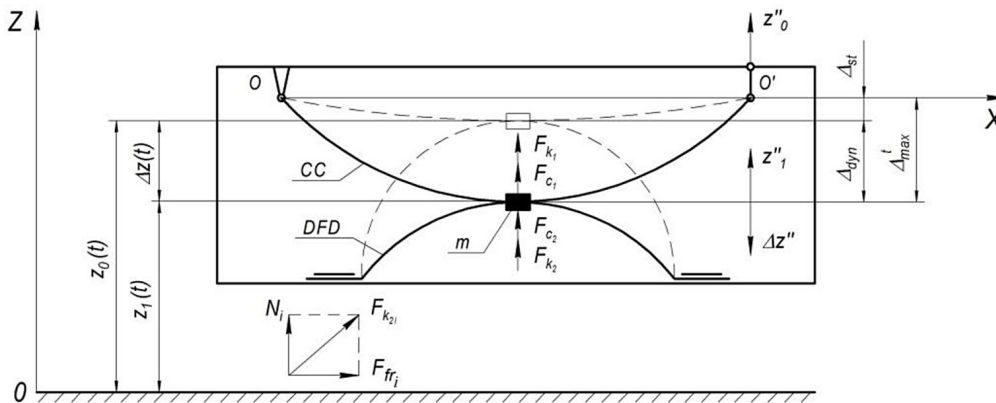
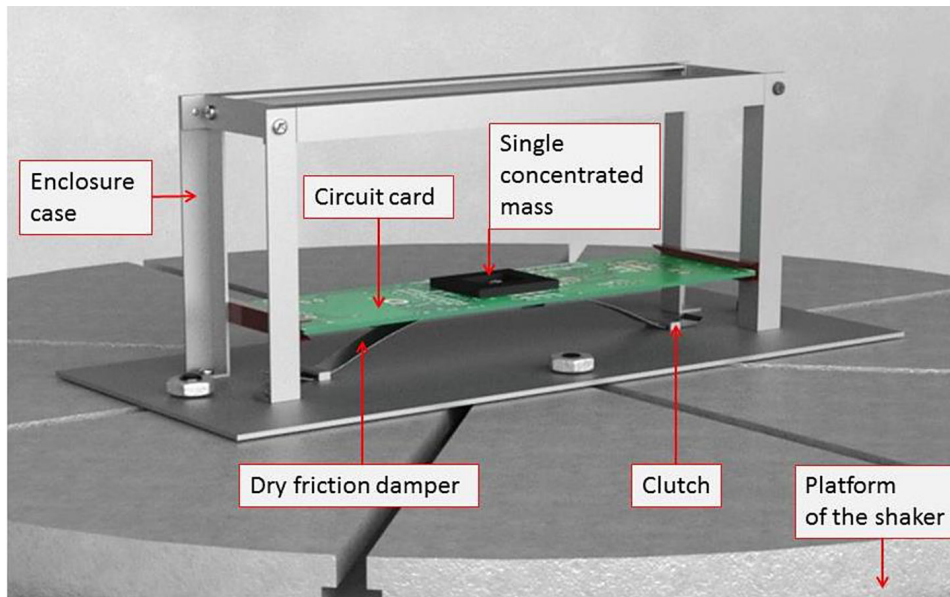


Figure 1. Dry friction damper embedded to circuit card in enclosure case: (a) experimental setup; (b) oscillatory model

where  $Z_0$  – amplitude;  $\omega$  – angular frequency;  $t$  – time;  $\varphi$  – phase of harmonic oscillation. Absolute acceleration of the mass  $m$  in inertial frame of reference is expressed as:  $z''_1 = -\Delta z'' + z''_0$ . Therefore equation of motion in non-inertial frame of reference represented by supports of circuit card  $O$  and  $O'$  looks analogically to [9]:

$$m\Delta z'' + F_{k1} + F_{k2} + F_{c1} + F_{c2} = mz''_0 \quad (1)$$

where:  $m\Delta z''$  – relative and  $mz''_0$  – fictitious forces of inertia;  $F_{k1}$  and  $F_{k2}$  – elastic restoring forces produced by CC and DFD correspondently;  $F_{c1}$  and  $F_{c2}$  – damping forces in materials of CC and DFD correspondently.

Generalized restoring force  $F_{k2}$  of DFD, acting when its both ends slip in the clutches, is the

net force of two reactions:  $N_i$  – vertical reaction equal to pressure from DFD and  $F_{fri}$  – horizontal reaction – friction force resisting slippage of the DFD ends in the clutch. The net force in each clutch is expressed as:

$$F_{k2i} = \sqrt{N_i^2 + F_{fri}^2} \quad (2)$$

The generalized force:

$$F_{k2} = \sqrt{N^2 + F_{fr}^2} \quad (3)$$

where:  $N = \sum_i N_i$ ;  $F_{fr} = \sum_i F_{fri}$ .

Due to insignificant influence of motion velocity the dry friction force is defined by Coulomb formula:

$$F_{fr} = \mu_{fr} N \quad (4)$$

where:  $\mu_{fr}$  – kinetic friction specified by friction pair;  $N$  – pressure between contacting surfaces.

Then substituting Eq. 4 into Eq. 3 gives:

$$F_{k_2} = N\sqrt{1+\mu_{fr}^2} \quad (5)$$

Since the pressure from DFD onto the clutch depends on its deflection  $\Delta z$  and stiffness  $k_2$ , then  $N = k_2\Delta z$ , and Eq. 5 becomes:

$$F_{k_2} = k_2\Delta z\sqrt{1+\mu_{fr}^2} \quad (6)$$

Then equation of motion (1) is expressed as:

$$m\Delta z'' + k_1\Delta z + k_2\Delta z\sqrt{1+\mu_{fr}^2} + c_1\Delta z' + c_2\Delta z' = mz_0''$$

or:

$$\ddot{q} + q(\omega_{01}^2 + \omega_{02}^2\sqrt{1+\mu_{fr}^2}) + 2n\dot{q} = Z_0\omega^2\sin(\omega t) \quad (7)$$

where:  $q = \Delta z(t)$ ;  $n = (c_1 + c_2) / 2m$  – total descent rate, where  $c_1, c_2$  – damping coefficients of CC and DFD correspondently;  $\omega_{01} = \sqrt{k_1/m}$  and  $\omega_{02} = \sqrt{k_2/m}$  – natural frequencies, where:  $k_1, k_2$  – stiffness of CC and DFD correspondently;  $Z_0$  – equation of motion (7) is analogical to [9] so its solution represents oscillation amplitude, which describes maximal dynamic deflection of the beams  $\Delta_{dyn}^{max}$  with respect to static equilibrium position  $\Delta_{st}$  in the oscillatory system (Fig. 1):

$$\Delta_{dyn}^{max} = \frac{Z_0\omega^2}{\sqrt{(\omega_{01}^2 + \omega_{02}^2\sqrt{1+\mu_{fr}^2} - \omega^2)^2 + (2n\omega)^2}} \quad (8)$$

For resonant oscillation ( $\omega = \omega_0$ ):

$$\Delta_{dyn}^{max} = \frac{Z_0\omega_0^2}{\sqrt{(\omega_{02}^2\sqrt{1+\mu_{fr}^2} - \omega_{02}^2)^2 + 4n^2\omega_0^2}} \quad (9)$$

where:  $\omega_0 = \sqrt{\omega_{01}^2 + \omega_{02}^2}$  – natural frequency of oscillatory system.

The effectiveness of dry friction damper to reduce vibration of circuit cards depends on its elastic and dissipative parameters, among which assessment of stiffness  $k_2$  attracts the most attention. With sufficient accuracy for practice, the stiffness of a curved beam can be determined in the same way as for a linear beam Eq. 10. On condition that damper contacts the center of circuit card the

stiffness of both beams ( $i = 1, 2$ ) are defined in accordance to [9] by the formula:

$$k_i = \frac{48E_iJ_i}{l_i^3} \quad (10)$$

where:  $E$  – young's modulus;  $J = bh^3/12$  – moment of inertia in cross-sectional area of the beam;  $l, b$  and  $h$  – length, width and thickness of the beam correspondently.

Dynamic deflection is produced by dynamic force:

$$P_1 = k_1\Delta_{dyn}^{max} \quad (11)$$

Maximal internal bending moment is produced by force  $P_1$  in central cross-section of circuit card:

$$M_1^{max} = P_1\frac{l_1}{4} \quad (12)$$

Functional dependence of maximal dynamic stress in circuit card Eq. 8 on DFD stiffness in resonance condition is expressed as:

$$\sigma_{dyn}^{max}(k_2) = Z_0\frac{k_1+k_2}{m}\frac{1}{\sqrt{\frac{k_2^2}{m^2}(\sqrt{1+\mu_{fr}^2}-1)^2 + 4n^2\frac{(k_1+k_2)}{m}}}\frac{l_1}{4}W_{i\bar{i}} \quad (13)$$

where:  $W_{oc} = bh^2/6$  – section modulus in bending.

Functional dependence of maximal dynamic deflection of circuit card Eq. 9 on DFD stiffness in resonance condition is expressed as:

$$\Delta_{dyn}^{max}(k_2) = Z_0\frac{k_1+k_2}{m}\frac{1}{\sqrt{\frac{k_2^2}{m^2}(\sqrt{1+\mu_{fr}^2}-1)^2 + 4n^2\frac{(k_1+k_2)}{m}}} \quad (14)$$

In condition of constant dynamic force acting with amplitude  $P_0 = const$  provided by constant vibration acceleration  $a_0 = Z_0\omega_0^2$ , functions Eq. 13 and Eq. 14 are expressed as:

$$\sigma_{dyn}^{max}(k_2) = P_0\frac{1}{\sqrt{k_2^2(\sqrt{1+\mu_{fr}^2}-1)^2 + 4n^2m(k_1+k_2)}}\frac{l_1}{4}W_{i\bar{i}} \quad (15)$$

$$\Delta_{dyn}^{max}(k_2) = P_0\frac{1}{\sqrt{k_2^2(\sqrt{1+\mu_{fr}^2}-1)^2 + 4n^2m(k_1+k_2)}} \quad (16)$$

Figure 2 represents graphs of Eq. 15 and Eq. 16 at  $a_0 = 10 \text{ m/s}^2$ . Physical and mechanical parameters of circuit cards and DFD were found by analytical and experimental method of sample parameters [10] and represented in Table 1. In this method based on solving the reverse strength problems strain and displacement, which are normally found by calculations, are, instead, measured experimentally and considered as given values for calculation of physical and mechanical

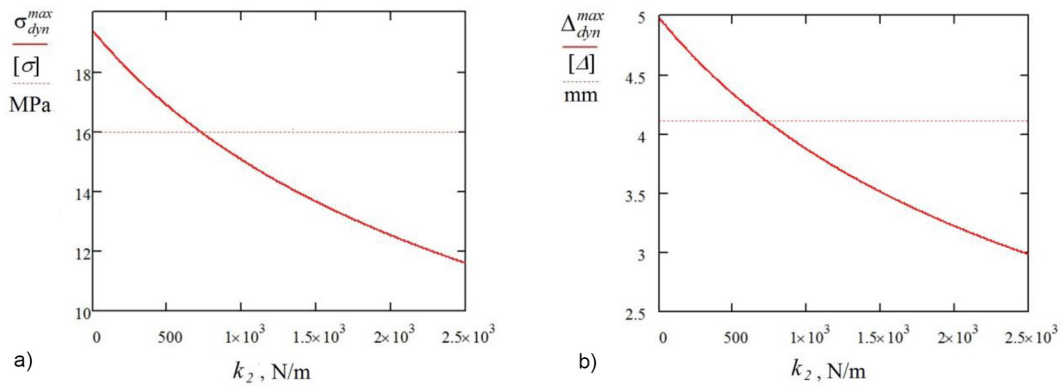


Figure 2. Dependences maximal dynamic stress (a) and deflection (b) of circuit card on DFD stiffness when  $\omega = \omega_0$  and  $P_0 = \text{const}$

parameters, which are then used in analytical modeling. Represented dependences are correspondent to first critical frequency of the main mode of oscillation what, as described in previous research [10], causes maximal magnitudes of stress and deflection in critical cross-section of circuit cards. Graphs in Figure 2 demonstrate gradual decline of stress and deflection due to increasing stiffness of DFD. Thus, in accordance to mathematical model Eq. 13 embedding elastic and dissipative joint in form of the dry friction damper should provide effective reduction of stress and deflection in critical cross-section of circuit card.

Obtained results were supported by using method for simulation modeling oscillation of circuit card with dry friction damper. Acting forces

and parameters of oscillatory system were taken identical to those used in mathematical modeling. Figure 3 represents designed in Simscape Multibody [12, 13] oscillatory system simulation model, which simulates motion of flexible circuit card and flexible dry friction damper.

“Motion” unit generates vertical motion of enclosure case and circuit card with acceleration  $10 \text{ m/s}^2$ . The generalized Simulink signal  $[z, z', z'']$ , where  $z$  – displacement;  $z'$  – velocity;  $z''$  – acceleration, is transmitted to “Joint Actuator” unit. “Joint Actuator” unit activates “Prismatic Joint” unit. “Support” unit represents rigid joint of base and side walls, which through supports “Revolute Joint” and “Custom Joint 1” support flexible circuit card (“Flexible Plate” unit).

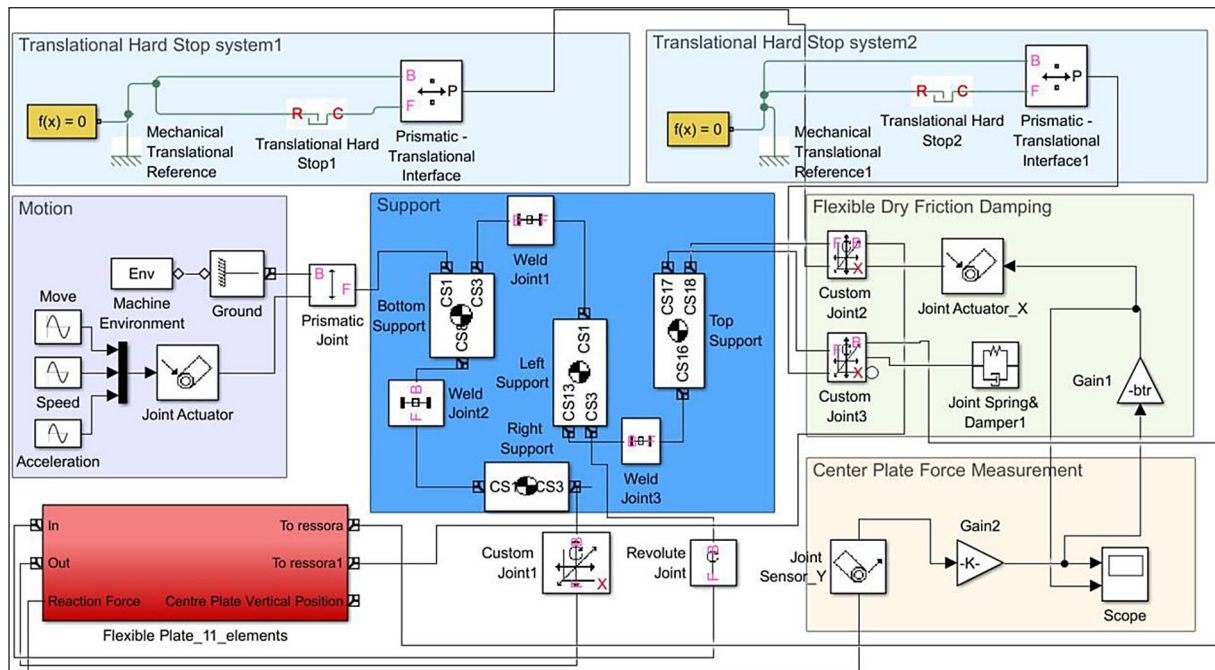


Figure 3. Simscape Multibody oscillatory model simulation for circuit card and dry friction damper

“Revolute Joint” has single degree of freedom – revolution around OY axis, “Custom Joint 1” has two degrees of freedom – revolution around OY axis and translational movement along the OX axis. Circuit card is modeled by the set of 11 flexible elements.

Dry friction damper is simulated by vertical spring with stiffness  $k_z$  and two dampers. First damper of the “Joint Spring & Damper 1” unit simulates viscous damping for DFD material with damping force  $c_z \Delta z$  in the support “Custom Joint 3”. Second damper simulates dry friction in the support “Custom Joint 2” with friction force  $F_{fr}$ . Both supports represent joint between damper and circuit card. “Central Plate Force Measurement” unit measures normal reaction  $N$  (contact pressure) in the contact spot between circuit card and damper (in the center of the card). “Flexible Dry Friction Damping” unit calculates dry friction force  $F_{fr}$ , proportional to reaction  $N$ . “Translational Hard Block System” units constrain motion of damper contact point on the OX axis.

Simulation formulates and solves equations of motion for all mechanical system. Displacement and stress of card center are measured by “Body Sensor” and “Joint Sensor” units from Simcape Multibody Library (not shown in Fig. 3). Simulation resulted in dependences of dynamic stress and deflection in critical cross-section of circuit card on DFD stiffness in condition of resonant excitation. Dependences are demonstrated by the graphs shown in (Fig. 4), which, in purpose of comparison, represents graphs obtained by both simulation and mathematical modeling. Comparing graphs obtained by mathematical modeling (Fig. 2) and simulation (Fig. 4) testified of their similar shape

and negligible deviation in absolute values – in particular the minimal acceptable limit of DFD stiffness differed by 6.9%.

### DRY FRICTION DAMPER DESIGN

There are known technologies [6, 7, 14] designed to reduce vibration amplitude either by increasing stiffness of circuit cards or by applying viscous damping mechanisms. Increasing stiffness of circuit cards by rigid fixing to an enclosure case and by rigid fixing enclosure case to the platform, or embedding to circuit card design a stiffener to reduce its deformation are supposed to increase their mass and size and do not exclude circuit card oscillation since they copy oscillations of enclosure case and then transmit them to installed electronic components what may cause mechanical damage especially in resonance condition.

Damping mechanisms normally [14] integrate viscous and elastic materials to the circuit card design. Nevertheless such modifications are not applicable to circuit cards, which are already manufactured. Moreover viscous and elastic dampers are insufficiently effective to fight vibration with frequency over 50 Hz, their specific orientation is too complex and they are temperature dependent and cumbersome.

There is known an appliance [15] that is the most similar by technical application and results to the offered one. In this appliance damping is provided by embedding flexible elements, which are wires and cables mounted by through-hole technology, to a circuit card. Vibration energy is dissipated due to deflections of different materials in flexible elements and friction between

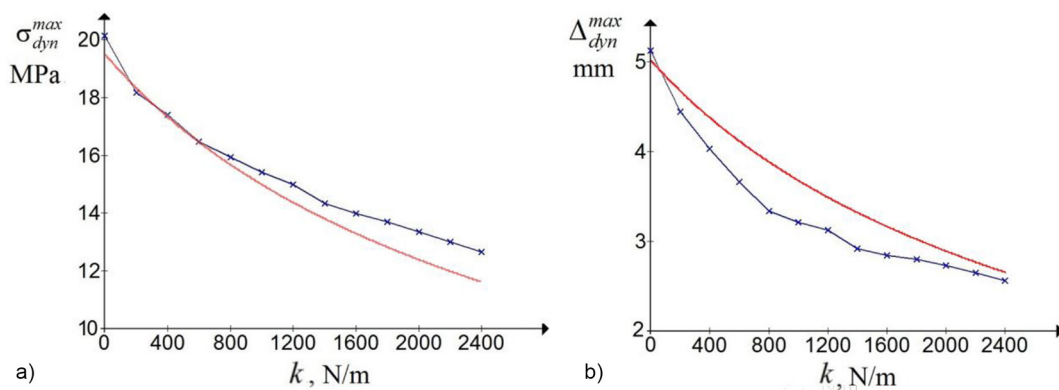


**Figure 4.** Comparison of graphs obtained by simulation (blue) and mathematical modeling (red): dependences of maximal dynamic stress (a) and deflection (b) in critical cross-section of circuit card with DFD on DFD stiffness in condition of resonant excitation

them. Nevertheless technical specification, design and estimating effectiveness for such appliance becomes difficult because of varying properties of used materials and unpredictable friction forces emerged.

DFD design made as semi-elliptical beam with rectangular profile is introduced by three variants shown on blueprints in Figure 5.

In accordance to Eq. 15 and Eq. 16 effectiveness to reduce dynamic stress and deflection in critical cross-section of circuit card in resonance condition depends on elastic and dissipative characteristics of DFD in particular on its stiffness. DFD stiffness is directly proportional to the restoring force  $F_{k2}$ , which produces pressure on the clutch and force opposite to friction force that resists damper slipping in the clutch. So, growing mentioned forces, as vibration amplitude increases, results in reducing dynamic stress and deflection transmitted to CC.

Developed mathematical model Eq. 17 specifies minimal limit value of the stiffness, which

provides compliance with strength and stiffness standard for circuit cards and is used in engineering calculations to determine geometric parameters for DFD designed as semi-elliptical beam with rectangular profile:

$$k_{min} = \frac{\sqrt{4n^4m - (\sqrt{1 + \mu_{fr}^2} - 1)^2 \left( 4n^2mk_1 - \left( \frac{P_0k_1l_1}{4W_{in}[\sigma]} \right)^2 \right)} - 2n^2m}{(\sqrt{1 + \mu_{fr}^2} - 1)^2} \quad (17)$$

Calculation is performed on the base of using specified parameters for circuit card and dry friction damper, which are:  $k_1$ ;  $m$ ;  $W_{oc}$ ;  $l_1$ ;  $n_1$ ;  $n_2$ ;  $\mu_{fr}$  and  $P_0$ . According to functions Eq. 15 and Eq. 16 increasing DFD stiffness gradually reduces stress and deflection in circuit cards. Obviously, reaching a critical maximal level (absolute stiffness) CC center displacement will be blocked, then  $\Delta_{dyn}^{max} = 0$  and  $\sigma_{dyn}^{max} = 0$  under dynamic force though. In this case DFD becomes a rigid support, which divides a given oscillatory system into two other systems with their own masses, elastic and

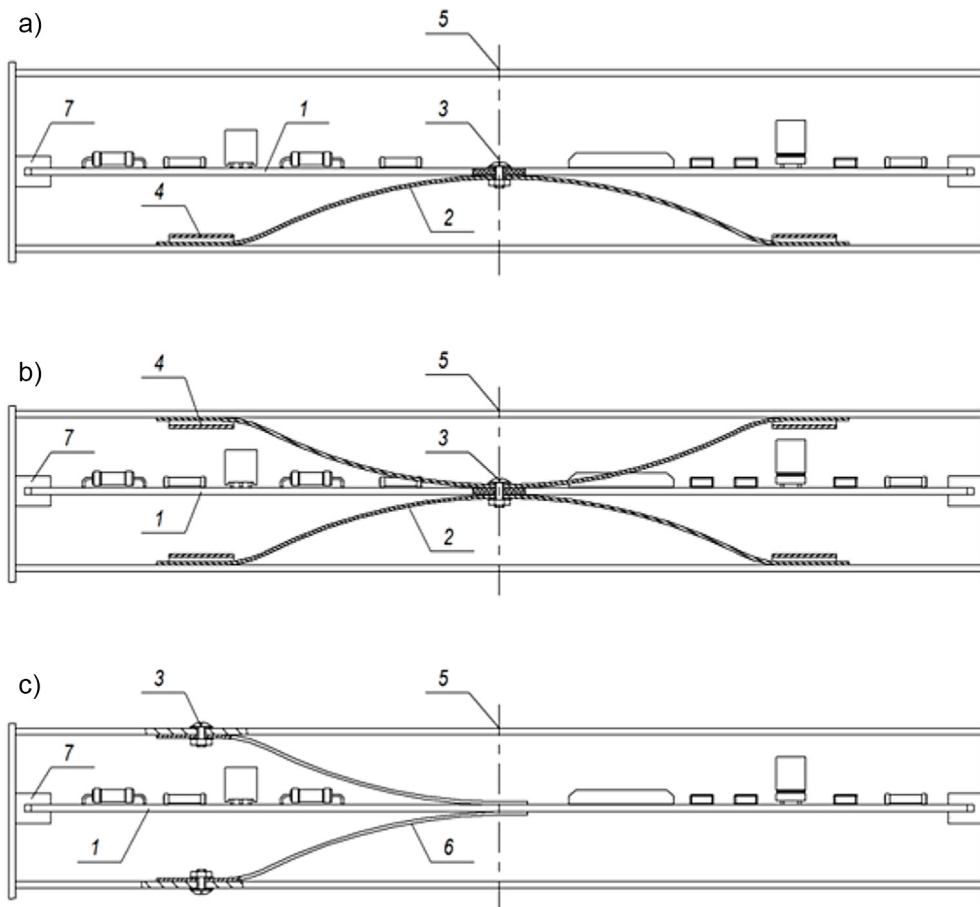


**Figure 5.** Dry friction damper designs introduced by semi-elliptical beam with rectangular profile: (a) beam; (b) double beam; (c) half-beam. 1 – circuit card; 2 – dry friction damper as curved beam; 3 – fitting; 4 – clutch; 5 – enclosure case; 6 – dry friction damper as curved half-beam; 7 – CC fixtures

dissipative parameters, natural frequencies and main modes of oscillation with other magnitudes of maximal stress and deflection. The critical stiffness is a supreme number what means  $\Delta_{dyn}^{max} \rightarrow 0$  or  $\sigma_{dyn}^{max} \rightarrow 0$  when:  $k_2 \rightarrow \infty$ . Therefore upper limit of the stiffness range can be recommended as maximal limit value calculated by formula Eq. 17 with respect to specified minimal limit value for stress or deflection.

Construction parameters of DFD, which are length, width and thickness, are to be calculated by formula Eq. (10) with respect to Young’s modulus  $E_2$  for the specified material of DFD. DFD effectiveness is provided by increasing its stiffness and also damping descent rate  $n_2$  and friction  $\mu_{fp}$ , which in turn depends on materials and surfaces in kinematic friction pair: DFD 2 (Fig. 5a; 5b) or 6 (Fig. 5c) and clutch 4 (Fig. 5). Nevertheless, providing and specifying these parameters are complicated in real design. Therefore recommendation is to use their minimum reference values [10] so possible error in calculation would contribute the safety factor. DFD design is introduced by three variants (Fig. 5) in order to propose variety of the design, all of them perform their function in the same manner though. The choice of the design remains for consideration

in favor of application to certain electronic package, circuit card layout etc.

### EXPERIMENTAL VERIFICATION OF DRY FRICTION DAMPER EFFECTIVENESS

Experimental vibration tests on circuit cards equipped with dry friction damper installed by the blueprint (Fig. 5a) were conducted on the shaker WEDS-200. DFD stiffness  $k_{min} = 718.75$  N/m was calculated by formula Eq. 17 using physical and mechanical parameters of circuit card and DFD (Table 1). This limit value was used to determine geometric parameters of DFD: 160×10×0.75 mm. Physical and mechanical parameters of circuit card and dry friction damper were found by method for sample parameters [10]. Maximal normal stress in surface layers of the circuit card was calculated by the Hooke’s law [10]. Strain was measured by strain gauge set on the CC surface in the place of concentrated mass – in the center of circuit card. Signal from strain gauge was sent to electrotenometry system.

Maximal deflections were read from vibration sensor set in the center of circuit card. Second vibration sensor attached to fixtures on the

**Table 1.** Physical and mechanical parameters of circuit card and dry friction damper

Objects	Dimensions, mm	Material	E, GPa	[σ], Pa	n, 1/s	m, kg	μ <sub>f</sub>
Circuit card	180 × 50 × 1.5	Glassfiber	14	16	5.48	0.05	0.2
Dry friction damper	160 × 10 × 0.75	Carbon steel	200	–	0.1	–	

**Table 2.** Maximal dynamic stress and deflection in circuit cards with and without dry friction damper embedded in the first critical frequency

Parameters	ω <sub>0</sub> , rad/s	σ <sub>dyn</sub> <sup>max</sup> , MPa	Δ <sub>dyn</sub> <sup>max</sup> , mm
Object			
Circuit card with dry friction damper	Experimental data		
	198.5	15.08	3.52
	Simulation data		
	233.4	16.14	3.46
	Mathematical modeling data		
	216.29	16.00	4.11
Circuit card	Experimental test data		
	163.1	18.96	4.75
	Simulation data		
	176.9	19.06	5.02
	Mathematical modeling data		
	180	19.71	5.07

shaker was reading oscillations generated by the shaker. Signals from two vibration sensors ABC 032 were sent to vibration analysis system. Generated oscillation with fixed frequencies were monitored by sound generator. Resonance frequencies were detected by method of floating frequency. Vibration tests were conducted under constant dynamic force with amplitude  $P_0$  produced by constant vibration acceleration  $a_0 = 10 \text{ m/s}^2$ . Strain gauges and vibration sensors were attached to unloaded circuit card before installing it into enclosure case and on the shaker. Maximal dynamic stress  $\sigma_{dyn}^{max}$  and maximal dynamic deflections  $\Delta_{dyn}^{max}$  were measured in the first critical frequency  $\omega_0$ . Table 2 represents mean values obtained as results of 5 repeated vibration tests and results of mathematical and simulation modeling for two groups of circuit cards – with and without dry friction damper embedded.

Comparing maximal magnitudes of dynamic stress and deflection obtained by experimental tests with results of simulation and mathematical modeling indicates of their similarity and slight relative difference from 6.1 to 16.8%, what approves sufficient accuracy of mathematic model Eq. 17 whereby possible difference can be used as safety factor. Comparative analysis of maximal magnitudes of dynamic stress and deflection obtained by vibration tests on two types of circuit cards – with and without dry friction damper embedded indicated significant relative reduction of these parameters by 20.5% and 25.9% correspondently. Achieved effect provides compliance with strength and stiffness standard for circuit card and approves application of DFD to reduce maximal dynamic stress and deflection in critical cross-section of circuit cards undergoing inertial resonant excitation.

## CONCLUSIONS

The mathematical model has been developed for estimation of maximal dynamic stress and deflection in critical cross-section of circuit card with embedded dry friction damper at critical frequencies. Functional dependences of maximal dynamic stress and deflection of circuit card on dry friction damper elastic and dissipative parameters, in particular on its stiffness have been revealed. DFD stiffness is directly proportional to the restoring force, which produces pressure on the clutch and force opposite to friction force that

resists damper slipping in the clutch, so, growing mentioned forces, as vibration amplitude increases, result in reducing dynamic stress and deflection transmitted to CC.

Developed mathematical model specifies minimal limit value of the stiffness, which provides compliance with strength and stiffness standard for circuit cards and is used in engineering calculations to determine geometric parameters for DFD designed as semi-elliptical beam with rectangular profile. DFD to be embedded to circuit card inside the enclosure case of electronic package is introduced by three variants of design.

The effectiveness of dry friction damper has been demonstrated by significant relative reduction of maximal magnitudes of dynamic stress and deflection by 20.5% and 25.9% correspondently. Effect has been demonstrated on circuit cards subjected to inertial resonant excitation.

## REFERENCES

1. Loon K., Kok C., Mohd E., Ooi C. Modeling the Elastic Behavior of an Industrial Printed Circuit Board Under Bending and Shear. *IEEE Transactions on Components, Packaging and Manufacturing Technology*. 2019. 9(1): 669–676. DOI: 10.1109/TCPMT.2018.2882575.
2. Allaparthi M., Khan M., Teja B. Three-dimensional finite element dynamic analysis for micro-drilling of multi-layered printed circuit board. In: *Materials Today, Proc.* 5(2): 2018, 7019–7028. DOI:10.1016/j.matpr.2017.11.365.
3. Cevdet N., Withers P., Murray C. Stresses in Micro-electronic Circuits. Reference Module in Materials Science and Materials Engineering. 2016. 12(1): 156–168. DOI:10.1016/B978-1-84569-528-6.00010-1
4. Wong E-H., Mai Y-W. Dynamic deformation of a printed circuit board in drop-shock in robust design of microelectronics assemblies against mechanical shock, temperature and moisture. Woodhead Publishing. 2015. 10: 327–378. DOI:10.1016/B978-1-84569-528-6.00010-1
5. Kim Y. Lee S-M., Hwang D-S., Seohyun J. Analyses on the large size PBGA packaging reliability under random vibrations for space applications. *Microelectronics Reliability*. 2020. 109. DOI:10.1016/j.microrel.2020.113654
6. Jouneghani K., Hosseini M., Rohanimanesh M., Dehkordi M. Dynamic behavior of steel frames with tuned mass dampers *Advances in Science and Technology. Research Journal*. 2017. 11(2): 146–158. DOI:10.12913/22998624/70763.

7. Veeramuthuvel P., Sairajan K., Shankar K. Vibration suppression of printed circuit boards using an external particle damper. *Journal of Sound and Vibration*. 2016. 366: 98–116. <https://doi.org/10.1016/j.jsv.2015.12.034>.
8. Boiko J., Kovtun I., Petrashchuk S. Vibration transmission in electronic packages having structurally complex design. *Proceedings of the First Ukraine IEEE international Conference on Electrical and Computer Engineering. UKRCON – 2017*. Kiev. 2017: 514–517. DOI: 10.1109/UKRCON.2017.8100294.
9. Kovtun I., Boiko J., Petrashchuk S. Mathematical model for dynamic force analysis of printed circuit boards. *Journal of Physics: Conference Series. The First International Conference on Advances in Smart Sensor, Signal Processing and Communication Technology. ICASSCT 2021*. Goa. 2021. DOI 10.1088/1742-6596/1921/1/012120.
10. Kovtun I., Goroshko A., Petrashchuk S. Mathematical modeling of stress in circuit cards represented by mechanical oscillatory systems. *Advances in Science and Technology Research Journal*. 2022. 16(1): 303–315. DOI: <https://doi.org/10.12913/22998624/144574>.
11. Pisarenko G.S., Kvitka O.L., Umanskiy E.S. *Strength of materials*. Kiev: Highest school. 2004. (in Ukrainian)
12. Chudnovsky V., Mukherjee A., Wendlandt J., Kennedy D. Modeling flexible bodies in simmechanics. *MatLab Digest*. 14(3): 2006.
13. Miller S., Soares T., Weddingen Y. Modeling flexible bodies with Simscape multibody software. *An Overview of Two Methods for Capturing the Effects of Small Elastic Deformations*. MathWorks. 2017.
14. Tae-Yong Park, Seok-Jin Shin, Sung-Woo Park, Soo-Jin Kang, Hyun-Ung Oh. High-damping PCB implemented by multi-layered viscoelastic acrylic tapes for use of wedge lock applications. *Engineering Fracture Mechanics*. 2021. 241. <https://doi.org/10.1016/j.engfracmech.2020.107370>.
15. Patent. UA 13063 C1 Ukraine, MPK: H05K 5/00, H05K 7/12, H05K 7/14. Electronic unit / V. P. Salnikov, E. P. Sereda : NVO «Khartron». – #95320384; publ. 28.02.1997; Bul. #1. (in Ukrainian)